Langmuir

Article

pubs.acs.org/Langmuir

Direct Comparison of Disaccharide Interaction with Lipid Membranes at Reduced Hydrations

Ben Kent,[†] Thomas Hauß,[†] Bruno Demé,[‡] Viviana Cristiglio,[‡] Tamim Darwish,[§] Taavi Hunt,[∥] Gary Bryant,[∥] and Christopher J. Garvey*[,§]

[†]Institute for Soft Matter and Functional Materials, Helmholtz-Zentrum Berlin, Hahn-Meitner-Platz 1, Berlin D-14109, Germany

[‡]Institute Laue Langevin, Grenoble 38000, France

[§]Bragg Institute, Australian Nuclear Science and Technology Organisation, Lucas Heights, NSW 2234, Australia

[∥]Centre for Molecular and Nanoscale Physics, School of Applied Sciences, RMIT University, Melbourne, VIC 3000, Australia

Supporting Information

ABSTRACT: Understanding sugar−lipid interactions during desiccation and freezing is an important step in the elucidation of cryo- and anhydro-protection mechanisms. We determine sucrose, trehalose, and water concentration distributions in intra-bilayer volumes between opposing dioleoylphosphatidylcholine bilayers over a range of reduced hydrations and sugar concentrations. Stacked lipid bilayers at reduced hydration provide a suitable system to mimic environmental dehydration effects, as well as a suitable system for direct probing of sugar locations by neutron membrane diffraction. Sugar distributions show that sucrose and trehalose both behave as typical uncharged solutes, largely excluded from the lipid bilayers regardless of sugar identity, and with no correlation between sugar distribution and the lipid headgroup position as the hydration is changed. These results are discussed in terms of current opinions about cryo- and anhydro-protection mechanisms.

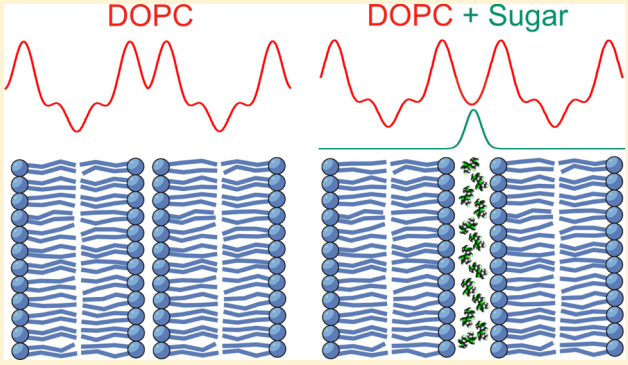

INTRODUCTION

Sugars, particularly disaccharides, are widely recognized for their ability to protect cellular membranes in environments with scarce liquid water. In the regimes of drying and freezing by slow cooling, which are mechanistically equivalent,[1] sugars are observed to be associated with tolerance to dry and cold environmental conditions.[2−7] Both of these environments involve an efflux of water from cells. During desiccation, removal of water external to the cells leads to a concentration of solutes in the extracellular solvent, and water effluxes from the cells until the osmotic gradient across the cell membrane returns to zero. In the case of slow cooling, slow enough to allow sufficient time for water concentrations to respond to osmotic gradients, ice usually forms first in the extracellular solution, concentrating the solutes in the remaining liquid water and creating an osmotic gradient across the cell boundary in a similar way to desiccation. On the time scales of natural environmental changes, cryo- and anhydro-protection can therefore be considered together.

During dehydration, lipid bilayer membranes are forced into close proximity with neighboring membranes. It is generally assumed that a primary mechanism for maintaining membrane viability is the avoidance of deleterious phase transitions in the membrane, as the normal transport properties of a membrane are predominantly associated with the lamellar fluid phase.[8] Phase transitions which affect the partitioning between the intra- and extracellular compartments (e.g., lamellar to hexagonal phase transition[9]), or change the dynamic nature of the hydrophobic domain through more rigid lipid chain packing (lamellar fluid to gel phase transition[10]) are found to be inhibited by sugar molecules in both model systems and biological cells.[11,12]

Several molecular mechanisms have been proposed to explain the stabilization of the fluid lamellar phase and the protective mechanism of sugars. The water replacement hypothesis[4] suggests that a specific interaction between sugar molecules and lipid headgroups is the primary mechanism of protection. The effects of a particular disaccharide consisting of two alpha linked glucose units, trehalose, is suggested to have a superior efficacy as a protectant based on its ability to hydrogen bond with lipid head groups and replace smaller and more dynamic water molecules. The evidence for this interaction is based on both (indirect) experimental evidence[13−18] and molecular dynamics simulations.[19] An alternative mechanism for the effect has been suggested, ascribing a key role to nonspecific volumetric and osmotic effects of the sugars which

Received: June 11, 2015
Revised: July 28, 2015
Published: July 30, 2015

DOI: 10.1021/acs.langmuir.5b02127
Langmuir 2015, 31, 9134−9141

mediate the compressive stresses induced in membranes brought into close contact by dehydration.[3,20,21] This explanation is supported by a model which quantitatively predicts the hydration dependence of the fluid−gel transition temperature,[22] as well as (indirect) experimental evidence that sugars tend to be excluded from the regions close to the membranes.[23−26] Andersen et al.[27] have attempted to reconcile the two views with a concentration dependent explanation, where the water replacement mechanism is dominant at low sugar concentration, to be replaced in importance by nonspecific effects at higher sugar concentrations.

Note that the discussion above is relevant to moderate levels of dehydration/freezing where glass formation does not occur. The formation of glassy sugar solutions[28] is an additional but separate protective mechanism which occurs at lower hydrations and/or temperatures. The effects of sugars on the structure of aqueous solutions, and in particular the glass transition, have been studied in detail.[29−33] The related effects of glass formation on membranes is discussed in detail in references.[15,34−36] The remainder of this paper is concerned with conditions where glass formation does not occur.

Phenomenologically, these two sugar membrane protection theories differ in the predicted sugar concentration profile between bilayers: in the case of the water replacement hypothesis the sugar concentration should be enhanced at the interface between the water and lipid bilayer; by contrast in the case of the nonspecific volumetric based hypothesis, sugar molecules are likely to be more concentrated in the solvent phase constrained by the barrier of the bilayer. Small angle neutron scattering has shown that sugars partition unequally between lipid phases and coexisting excess solution phases, giving a mesoscopic view of the sugar location within lipid bilayer systems.[23] Recently[37] we have demonstrated how the membrane neutron diffraction technique[38−42] can be used to directly extract the density profile of sugar molecules in the aqueous layer between opposing lipid bilayers. It was shown, at a single sugar composition, that the density profile is a Gaussian centered in the water layer. This approach,[41] where the components of a fluid bilayer are decomposed into quasi-molecular fragments, and a Gaussian describes the probability of occupancy per unit length across the bilayer (Figure 1), was extended to extract the profile of the sugar molecules.

As lipid bilayer membranes are forced into close proximity due to dehydration, they form stacks of bilayers periodically interspersed with aqueous solution. This formation, effectively one-dimensional crystallites, is an ideal system to study by diffraction. By reconstructing the scattering density profiles of the system, the average position and distribution of components within the bilayer unit cell can be determined. Variation of the scattering contrast of the sugar (its neutron scattering length density (SLD)) by selective deuteration of its nonexchangeable hydrogens allows the sugars to be labeled and identified separately from the rest of the system. In this paper, we present the results of neutron membrane diffraction experiments into the locations of trehalose and sucrose within a DOPC bilayer system at reduced hydrations.

MATERIALS AND METHODS

Stacked Bilayers. Samples consisted of stacked bilayers of the unsaturated phospholipid dioleoylphosphatidylcholine (DOPC) on quartz slides. DOPC was used as purchased from Avanti Polar Lipids (Alabaster, AL). Deposition onto the substrate was achieved by dissolving DOPC in a chloroform/methanol mixture and spraying the sample evenly over the entire surface of the slide (65 × 25 mm^2). Spraying was performed with a low pressure regulated nitrogen supply and was performed over several minutes to prevent buildup of excess solvent on the slide surface. Trehalose or sucrose were incorporated by dissolving in methanol and adding this to the mixture prior to spraying. Any solvent remaining following deposition was removed by placing the samples in a vacuum for several hours. Sample quantities were determined gravimetrically following removal of all solvent. Samples averaged approximately 7 mg, corresponding to about 1500 bilayers, assuming an even coverage across the slide.

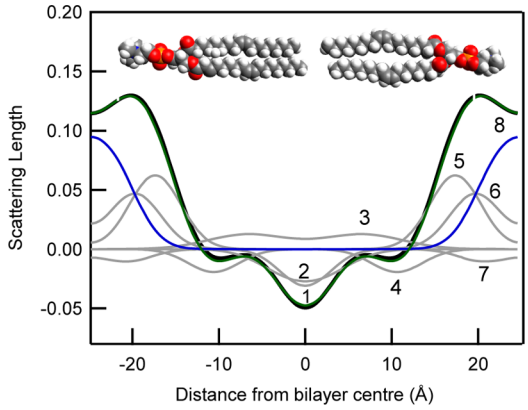

Figure 1. Bilayer centered scattering density profile of dioleoylphosphatidylcholine (DOPC) equilibrated at 57% RH (green line). A model fitted to this profile (black line) is the sum of the scattering densities (gray lines for lipid components, blue line for water) of the individual components of the unit cell: (1) terminal methyl group, (2) acyl group, (3) double bond, (4) acyl groups, (5) glycerol, (6) phosphorus, (7) choline, and (8) water.

Sample hydration was controlled by equilibrating the samples in chambers of known humidity (at a selected level of deuteration using an appropriate mixture of H_2O and D_2O) for at least 8 h. As water is absorbed from the gas phase, the lipids self-assemble into stacked bilayers. The trehalose/DOPC samples were measured at 0.063, 0.15, 0.21, and 0.50 sugars per lipid, while sucrose/DOPC samples were measured at 0.063, 0.21, and 0.50 sugars per lipid. For one value of relative humidity (57% RH), we compare sucrose and trehalose at several sugar/lipid ratios. The effects of different humidities, from 11% to 75% RH, were studied at a single trehalose/lipid ratio (0.5) and compared to DOPC without sugar.

Note that we are interested here in the mechanisms by which sugars protect membranes during desiccation. The hydrations studied here (where samples are equilibrated to relative humidities between 75% and 11%) range from mild to severe dehydration. Relative humidity of 75% corresponds to an osmotic pressure of −40 MPa,[43] and is equivalent to freeze dehydration at about −33 °C.[21] This is exactly the range that is of interest in cryobiology and anhydrobiology. So although conducting similar studies at higher hydrations may be of interest for other reasons, it is not very relevant to freezing or desiccation, or the effect of sugars in this range. This technique was chosen precisely because it can give such excellent results over the hydration ranges of interest.

Sugar Deuteration. Hydrogenated sugars, sucrose and trehalose (Figure 2), and the Raney nickel catalyst were purchased from Sigma-Aldrich, Inc. (St. Louis, MO). Deuterated trehalose with two different nonexchangeable deuterium abundances (67.8%D and 73.4%D) as well as deuterated sucrose (60.0%D) were prepared by catalytic exchange reactions following a procedure of Koch and Stuart[44,45] using a deuterated Raney nickel catalyst in D_2O. The percentage deuteration at each specific carbon site in sucrose and trehalose molecules was calculated by ^{1}H NMR by measuring the relative integrations of the residual proton signals of the exchanged proton sites and those which remain unexchanged (carbon-bound hydrogens vicinal to hydroxyl groups, i.e., C1,1′ C5,5′ in trehalose and C5 C1′C5′ in sucrose). Mass

DOI: 10.1021/acs.langmuir.5b02127
Langmuir 2015, 31, 9134−9141

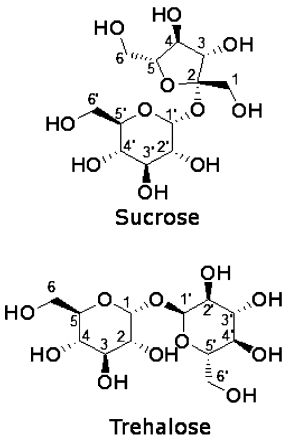

Figure 2. Two sugars considered in this study. Numbers indicate the sites of the unexchangeable hydrogens, deuterated as described in the text.

spectroscopy was utilized to confirm the overall isotopic purity of the molecule. Figures and spectra can be found in the Supporting Information.

Neutron Diffraction and Scattering Density Profile Reconstruction. Neutron diffraction data consists of intensity peaks (pseudo Bragg) caused by the constructive interference of scattered neutrons, superimposed upon a linear background signal. The angular, θ, position of the peaks is described by the Bragg equation:

$$2d \sin\theta = n\lambda \tag{1}$$

where d is the distance of the repeat spacing; n is an integral number, the order of the peak; and λ is the wavelength of the neutrons.

Scattering density profiles of the samples were reconstructed using Fourier synthesis.[46] The integral scattered intensities of the pseudo-Bragg peaks were determined by fitting Gaussian distributions of intensity over a linear background determined from the scattered intensity either side of the reflection. Structure factor magnitudes were calculated from these intensities after accounting for the Lorentz correction and an absorption correction using a model of an infinite plane of finite thickness,[47] to correct for the different path lengths of the scattered neutrons through the sample at different scattering angles:

$$f(h) = \sqrt{I(h)\, A(h) \sin\theta} \tag{2}$$

where $f(h)$ is the structure factor magnitude of the hth order, $I(h)$ is the scattered intensity, $A(h)$ is the absorption correction, and $\sin\theta$ is the Lorentz correction.

Neutron membrane diffraction was performed on the V1 membrane diffractometer at the Helmholtz-Zentrum Berlin (Germany) from samples of DOPC, trehalose/DOPC, and sucrose/DOPC, and on the D16 small momentum transfer diffractometer (Institut Laue-Langevin, Grenoble, France) from samples of DOPC and sucrose/DOPC. These instruments probe the appropriate angular range and hence repeat spacings for lipid bilayers through a combination of high angular resolution and long wavelength neutrons (cf. eq 1).

On the V1 instrument, the neutron wavelength was 4.56 Å. A 19 × 19 cm^2 area detector was used with a sample to detector distance of 1.0 m. Rocking curves of each of the first five pseudo-Bragg peak orders were recorded by positioning the center of the detector on the peak and rotating the sample relative to the incident neutron beam through a small angle around the maximum intensity for each peak. Samples were mounted vertically and sealed in an aluminum canister sample environment with the selected saturated salt solution at least 12 h prior to measurement. The salt solutions and humidities generated were 11% (lithium chloride); 33% (magnesium chloride); 57% (sodium bromide) and 75% (sodium chloride).[43] The temperature of the samples was fixed at 25 °C for all measurements.

On the D16 instrument, the wavelength was 4.7 Å. To optimize the incident neutron flux, the beam was vertically focused to the sample, and to optimize sample illumination and angular resolution in the horizontal direction two pairs of collimating slits were used. Diffraction patterns were collected using the Millimeter Resolution Large Area Neutron Detector (MiLAND), a high pressure ^{3}He neutron detector with an area of 320 mm × 320 mm and a "pixel" resolution of 1 mm × 1 mm. The sample-to-detector distance was 900 mm. Two overlapping detector positions were used, 13° and 30° to the incident beam, covering reflection orders 1−4 and 4−5, respectively. The incident angle of neutrons on the sample was varied continuously by rotating the sample through the angular ranges 1−12° and 10−18°, respectively, for each detector position. D16 measurements utilized a controlled humidity and temperature environment the operation of which is detailed elsewhere.[48] On both instruments diffraction orders higher than the fifth order were not detected above the background.

The SLD on a per lipid scale $\rho^*(z)$ is calculated from the structure factors by Fourier summation:

$$\rho^*(z) = \rho_0^* - \frac{2}{kd}\sum_{h=1}^{n} f(h)\left(\cos\frac{2\pi hz}{d}\right) \tag{3}$$

where z is the distance from the center of the bilayer, ρ_0^* is the product of the average SLD of the unit cell and the area per lipid, d is the repeat spacing, and k is an instrumental scaling constant.

Structure factor phases were determined by varying the SLD of the water layer between opposing lipid bilayers,[42] achieved by varying the D_2O/H_2O in the sample chamber. Scattering density profiles were scaled to number density per lipid. This is achieved by dividing the dimensionless absolute scattering density per lipid[42] by the difference in scattering lengths of one molecule of the labeled component at the higher and lower deuteration amounts. Further details on the structure factor phasing and scaling method can be found in the Supporting Information.

RESULTS AND DISCUSSION

Water distribution profiles and sugar distribution profiles were determined by subtraction of SLD profiles from the profiles of their corresponding higher-deuterated equivalent sample. Truncation artifacts, consisting of ripples in the difference profiles, can be observed due to the truncation of the Fourier series to the number of pseudo-Bragg peaks observed.[49] In all measurements, four or five pseudo-Bragg peaks were observed, and errors due to truncation artifacts were minimal. Typical diffraction curves are shown in Figure 3. To check whether

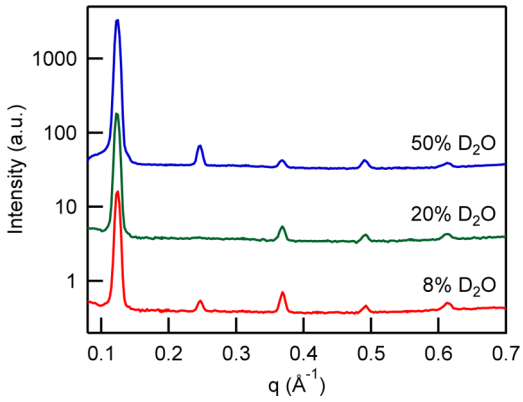

Figure 3. Diffraction data for 0.5 trehalose/DOPC equilibrated at 57% RH with three water contrasts (translated vertically for clarity). The area under the peak $[I(h)]$ goes through a minimum when the form factor $[f(h)]$ changes phase. This can be seen in the second peak, which changes phase between 8% D_2O and 50% D_2O (see Supporting Information Figure S1).

DOI: 10.1021/acs.langmuir.5b02127
Langmuir 2015, 31, 9134−9141

truncation artifacts were masking real differences due to deuterated labeled components in the system, difference profiles at each of the three D_2O/H_2O ratios were compared. In each case, the difference profiles were consistent while the background truncation artifacts varied. Sugar distribution profiles using the lower D_2O/H_2O ratios (0% or 8% D_2O) were used in the final analysis to maximize the difference in the SLD between the hydrogenated and deuterated sugars and the water layer.

To better focus on the water layer the remaining SLD profiles are shown centered on the middle of the water layer (rather than centered on the middle of the bilayer, as in Figure 1). Figure 4 shows an example scattering density plot of

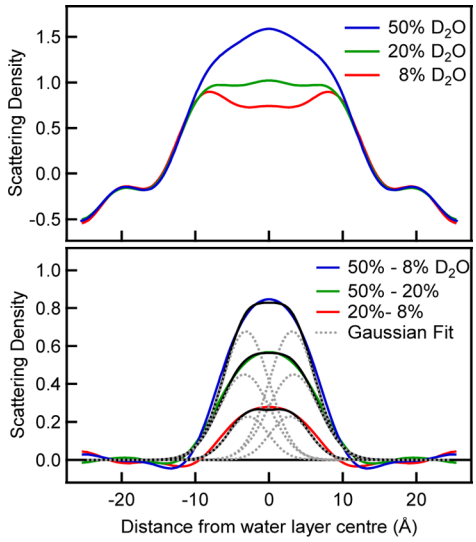

Figure 4. Water layer centered scattering density profiles for 0.5 trehalose/DOPC equilibrated at 57% RH (top) with three water contrasts. The lower panel shows the differences between these profiles, indicating the water distribution in the system. Each difference profile is fit by the sum (solid black line) of two Gaussian distributions (dotted black lines).

trehalose/DOPC at three measured D_2O/H_2O ratios, with their corresponding difference profiles showing the scattering density differences in the water layer due to the differences of the relative amounts of deuterium and hydrogen in the water layer. In regions in the system where there is no water, that is, within the DOPC bilayer, the scattering density profiles of the system are identical and the difference profiles are zero within errors. The integrated area of each water layer difference profile yields a total SLD difference equal to the SLD difference between the H_2O and D_2O of the two systems producing the difference profile. As the *y*-axis scattering density is scaled on a per-lipid basis, dividing the SLD total difference by the SLD difference of two water molecules of the same D_2O and H_2O ratios, the number of water molecules per lipid can be determined. Comparisons of this number from multiple difference profiles for each system provides an additional check of the scattering density scaling factors.

Figure 5 shows number density sugar and water distributions in each of the measured systems containing sugar. Also plotted for each system are the water distributions for an equivalent system in the absence of sugar. Sugar distributions have been multiplied by a factor of 10 for clarity.

For all systems, the water distributions are best fit by the envelope of two Gaussian profiles (cf. DOPC bilayers Figure 4 bottom). The double Gaussian form has been observed previously in a full deconvolution of the scattering length density profile of DOPC[41] and may be due to the slight densification of water hydrating the lipid headgroups.[50] By contrast to the two Gaussian distributions required to fit the water distribution, the distribution profiles of both sugars for all systems are best fit by a single Gaussian centered in the middle of the water layer.

The results show the qualitative differences between the sugar and water locations. At a constant 57% relative humidity (Figure 5 left and middle columns), the sugar distributions increase in area and amplitude as the sugar/DOPC ratio increases, reflecting the greater contrast between the hydrogenated and deuterated sugars at higher sugar concentrations. It is clear from the shape and location of the distributions that there is a propensity for the sugars to accumulate in the middle of the water layer. The sucrose distributions are comparatively broader when compared to the equivalent trehalose distributions, suggesting sucrose penetrates slightly further into the bilayer headgroup region than trehalose. While the trehalose distributions have the same form as sucrose, they follow a sharper Gaussian profile and show that trehalose is excluded from or has negligible concentration in the outer regions of the water distributions. This indicates that trehalose is not present in the water that penetrates furthest into the headgroup region of the lipid bilayer. It is also important to note that there is no explicit chemical detail in the quasi-molecular fragment model and it does not provide information on any preferred molecular orientation,

The highest sugar/lipid ratio of 0.5 sugars/lipid produces the largest and broadest sugar distributions. An increase to this sugar/lipid ratio coincides with a broadening in the water distribution, which is evident when comparing with the water distribution for the equivalent sugar-free system. While this change increases the repeat spacing of the lipid bilayer (Figure 6a), there is no evidence of an increase in the number of waters per lipid (Figure 6b). Instead, the volume of the sugar-water solution is greater in the system containing sugar than the volume of the water in the equivalent sugar-free system; therefore, there is an increase in the distance between opposing lipid headgroups and the repeat spacing with the addition of sugar at constant environmental conditions.

The absence of correlation between number of water molecules present and the bilayer repeat spacing can also be seen at lower sugar/lipid ratios. The clearest example of this is the jump in number of water molecules while the repeat spacing remains constant between the pure DOPC system and both the 0.063 sugars/lipid systems.

At low sugar/lipid ratios, the hydration (osmotic) effect of the sugar dominates—the presence of the sugar helps retain more water in the system at fixed RH,[51] increasing the number of waters per lipid and water distribution width but having little effect on the bilayer repeat spacing. This hydrating effect appears to be constant within the range of sugar/lipid ratios studied here.

At higher sugar/lipid ratios, the volumetric effects of the sugar dominate over the hydrating effects. The physical volume of the sugars increases the volume of the intrabilayer solution, further separating opposing lipid bilayers, with this effect increasingly evident as the sugar/lipid ratio is increased, and is the same general trend as found previously for hydrated

DOI: 10.1021/acs.langmuir.5b02127
Langmuir 2015, 31, 9134−9141

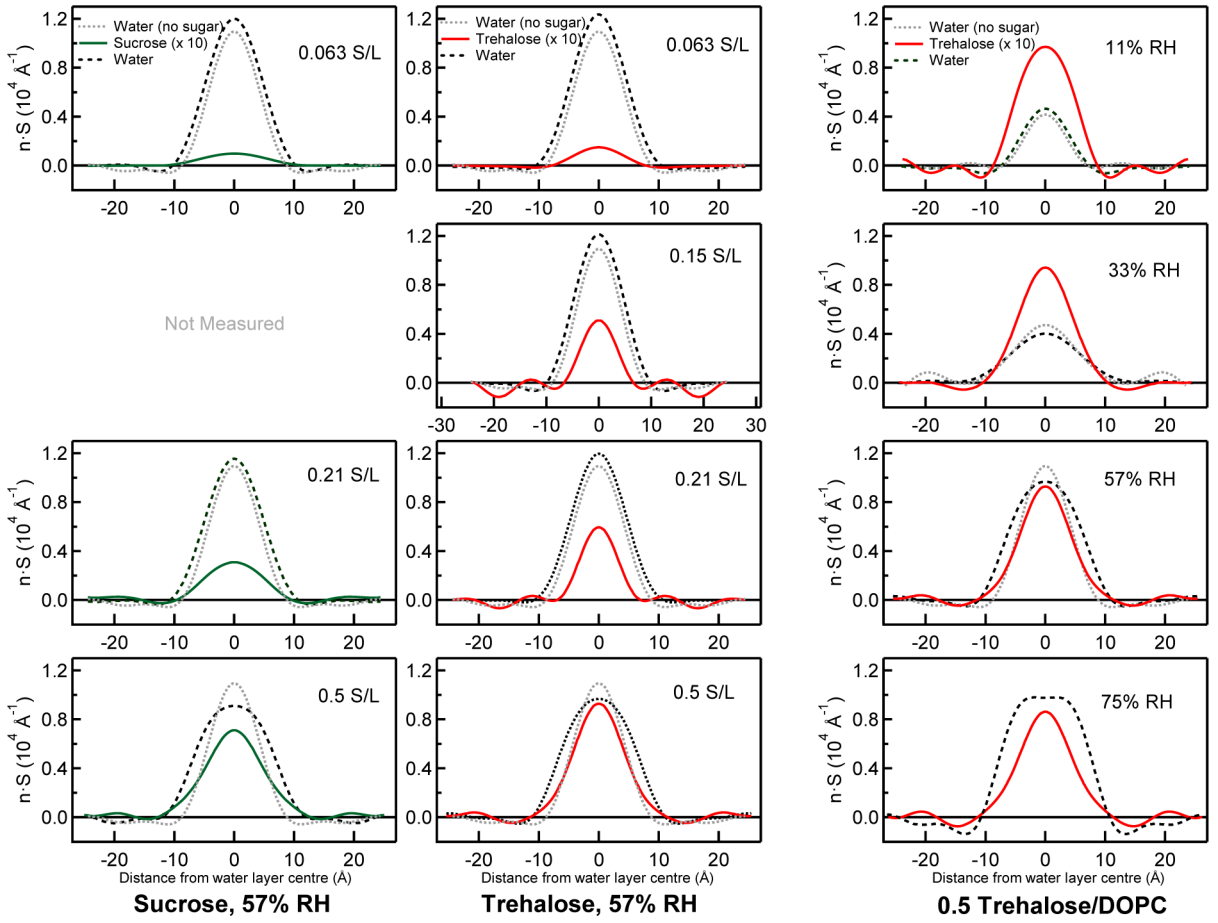

Figure 5. Sugar and water number densities per lipid as a function of the distance from the water layer center in bilayer DOPC systems. Sugar distributions have been multiplied by a factor of 10 for clarity. Left and middle columns: sucrose and trehalose in DOPC at various sugar/lipid (S/L) ratios at 57% RH. Right column: trehalose at 0.5 sugars/lipid for various relative humidities.

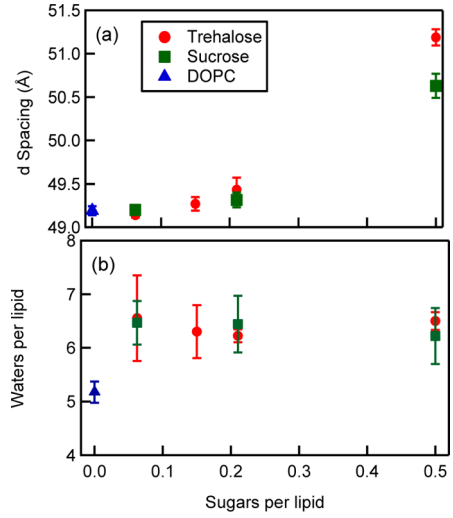

Figure 6. System parameters of DOPC, trehalose/DOPC and sucrose/DOPC as a function of sugar/lipid ratio: (a) Bilayer repeat spacing and (b) number of waters per lipid. All measurements at 57% RH.

lamellar phases.[22] Increasing this separation between bilayers reduces hydration forces acting on the bilayer,[20] and therefore reduces the possibility of phase transitions.

For a constant humidity, the results show that there is no propensity for the sugars to locate preferentially near the hydration shell of the DOPC headgroup, and consequently there is no evidence of a change in the shapes of the sugar distributions as the sugar ratio increases due to a sugar saturation effect surrounding the headgroup. The changes in the system parameters as the sugar/lipid ratio is changed provide direct evidence that the hydrating effects of sugars and the volumetric effects of sugars could account for observed cryo-protective effects of sugars.

This clear experimental result contradicts molecular dynamics (MD) simulations which have been cited as evidence for the water replacement hypothesis,[19,52] and the modifications to the water replacement hypothesis proposed by Westh et al.,[27,53] where after an initial enhancement of concentration in the headgroup region the effect is saturated, with the remainder of the saccharide molecules behaving as simple solutes in the intervening water bilayer.[54]

Turning now to the effect of hydration at constant sugar:lipid ratio, DOPC and 0.5 trehalose/DOPC samples were measured 11%, 33%, 57%, and 75% RH (Figure 5 right column). At 11% RH, the DOPC sample exhibited a qualitatively different scattering density profile to the other measurements (Figure 7 top), accompanied by a change in the bilayer repeat spacing. We attribute these features to the formation of a rhombohedral phase in this sample.[55] The presence of trehalose prevented this

DOI: 10.1021/acs.langmuir.5b02127
Langmuir 2015, 31, 9134−9141

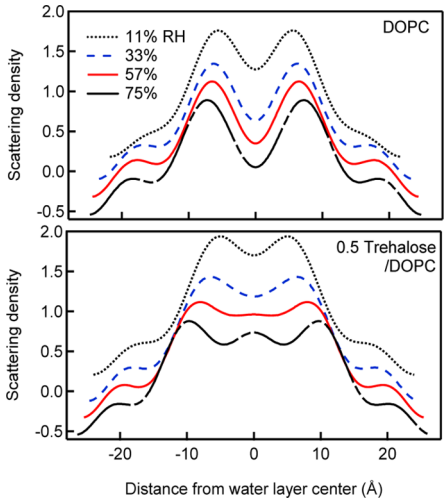

Figure 7. Water layer centered scattering density profiles for DOPC (top) and 0.5 trehalose/DOPC (bottom) for four relative humidities. A change in the bilayer profile at 11% RH for the DOPC sample is believed to be due to the formation of a rhombohedral phase.

phase formation, with all measurement consistent with a fluid lamellar phase.[56]

The trehalose distribution for 0.5 sugars/lipid remains similar for all relative humidities (Figure 5, right column). However, over the same RH range, there is a significant change in the water distributions, which increase in amplitude and width as the RH increases. This correlates with an increase in the number of waters per lipid as the RH increases (Figure 8b), and

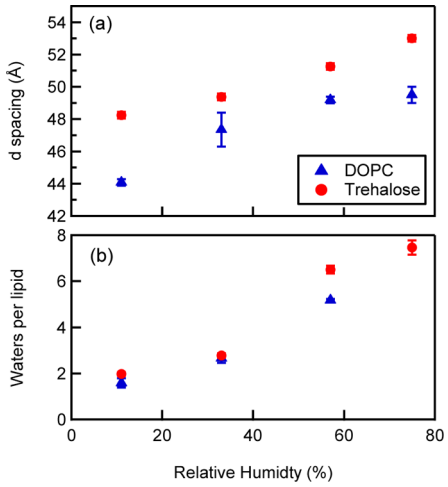

Figure 8. System parameters as a function of relative humidity for DOPC and 0.5 trehalose/DOPC: (a) *d* spacing and (b) number of water molecules per lipid.

causes an increase in the bilayer repeat spacing (Figure 8a) as the volume of the intrabilayer solution increases. The qualitatively different behaviors between the trehalose and water distributions as the RH changes indicates there is little correlation between the distribution of the sugar and the hydration of the system.

Adding trehalose increases the repeat spacing at each relative humidity. However, it is not until the RH is raised to 57% RH, that this increase is accompanied by an increase in the number of waters per lipid (note that the number of waters per lipid for DOPC at 75% RH was not measured). At the lower hydration of 33% RH, the increase in repeat spacing due to the presence of trehalose cannot be attributed to the hydrating properties of trehalose. Instead, the volumetric properties appear to dominate.

Significantly, these results show there is no correlation between the trehalose distribution and the position of the DOPC headgroups. As the relative humidity changes, the distance between opposing DOPC headgroups changes as the volume of solution between the bilayers changes. This can be observed in the increase in the repeat spacing and the increase in the water distribution area and width with increasing RH. During these changes, the location of the trehalose remains constant within errors. Such a result could not be expected if there was a relationship between the location of the trehalose and the position of the DOPC headgroups. These results clearly show trehalose acts in the same way as any nonspecific uncharged solute with no (significant) specific interaction with DOPC headgroups.

Finally, we again point out that the range of hydrations studied here is exactly the range of interest for desiccation and freezing damage of membranes.

Even though the distances between opposing bilayers are small, the sugars are concentrated in the center of the water layers, regardless of hydration. If specific interactions with the lipid headgroups were to play a major role, they would be distributed much more evenly across the water layer. Indeed, if the sugars were truly replacing the water, one would expect the number densities of sugar (Figure 5) to be broader than the number densities of the water. This is clearly not the case.

CONCLUSIONS

When examining the scattering density profiles of DOPC bilayer stacks we find that the presence of sugar has little effect on the bilayer itself for a given hydration, therefore the main changes are in the structure of the aqueous layer (Figure 5, right column). The fact that the sugar layer can be fit to a Gaussian profile centered in the middle of the water layer implies that the sugars are concentrated more in the center of the bilayer, rather than around the headgroups.

The basis of the water replacement hypothesis is that sugar molecules, most notably trehalose, are able to stabilize the area per lipid headgroup during dehydration[4,57] by replacing the more thermally mobile water molecules around the lipid headgroups. By examining the location and distribution profile of sucrose and trehalose as a function of sugar/lipid ratio at constant relative humidity, we have shown that there is no qualitative change to the sugar distribution as the sugar/lipid ratio increases. At constant sugar/lipid ratio, there is clearly no correlation between the sugar distribution and the position of the DOPC headgroups. Combined, these results show that sugars impart a cryoprotective effect on lipid bilayer membranes that is due to an increase in distance between opposing lipid bilayer headgroups due to the hydration and volumetric properties of the sugars, without specific interaction between the sugars and the lipids.

ASSOCIATED CONTENT

Supporting Information

The Supporting Information is available free of charge on the ACS Publications website at DOI: 10.1021/acs.langmuir.5b02127.

DOI: 10.1021/acs.langmuir.5b02127
Langmuir 2015, 31, 9134−9141

Structure factor phasing and scaling method, sugar deuteration method, and associated NMR spectra (PDF)

AUTHOR INFORMATION

Corresponding Author

*E-mail: cjg@ansto.gov.au.

Notes

The authors declare no competing financial interest.

ACKNOWLEDGMENTS

This research was supported by the Australian Research Council through Discovery Projects DP110105380 and DP0881009 and Linkage Project LP0884027, with additional financial support from BHP Billiton Worsley Alumina and Alcoa of Australia. This work was supported through the Australian Access to Major Research Facilities Fund (AMRF), and AINSE Grants 11173, 12024, and 13075. We thank the ILL and HZB for allocation of beamtime. The authors also acknowledge the use of NCRIS-supported National Deuteration Facility Laboratories for the synthesis of deuterated sugar molecules.

ABBREVIATIONS

SLD, scattering length density; DOPC, dioleoylphosphatidylcholine; %D, percent deuteration; RH, relative humidity

REFERENCES

(1) Storey, K. B. Organic solutes in freezing tolerance. *Comparative Biochemistry and Physiology a-Physiology* **1997**, *117* (3), 319−326.

(2) Billi, D.; Potts, M. Life and death of dried prokaryotes. *Res. Microbiol.* **2002**, *153* (1), 7−12.

(3) Bryant, G.; Koster, K. L.; Wolfe, J. Membrane behaviour in seeds and other systems at low water content: the various effects of solutes. *Seed Sci. Res.* **2001**, *11* (1), 17−25.

(4) Crowe, J. H.; Crowe, L. M.; Chapman, D. Preservation of Membranes in Anhydrobiotic Organisms: The Role of Trehalose. *Science* **1984**, *223* (4637), 701−703.

(5) Crowe, L. M.; Crowe, J. H.; Rudolph, A.; Womersley, C.; Appel, L. Preservation of freeze-dried liposomes by trehalose. *Arch. Biochem. Biophys.* **1985**, *242* (1), 240−247.

(6) Crowe, J. H.; Crowe, L. M.; Carpenter, J. F.; Wistrom, C. A. Stabilization of dry phospholipid bilayers and proteins by sugars. *Biochem. J.* **1987**, *242* (1), 1−10.

(7) Rolland, F.; Baena-Gonzalez, E.; Sheen, J. Sugar sensing and signaling in plants: Conserved and novel mechanisms. In *Annual Review of Plant Biology*; Annual Reviews: Palo Alto, 2006; Vol. *57*, pp 675−709.

(8) Singer, S. J.; Nicolson, G. L. Fluid Mosaic Model of Structure of Cell-Membranes. *Science* **1972**, *175* (4023), 720−731.

(9) Garvey, C. J.; Lenne, T.; Koster, K. L.; Kent, B.; Bryant, G. Phospholipid Membrane Protection by Sugar Molecules during Dehydration-Insights into Molecular Mechanisms Using Scattering Techniques. *Int. J. Mol. Sci.* **2013**, *14* (4), 8148−8163.

(10) Lenné, T.; Bryant, G.; Holcomb, R.; Koster, K. L. How much solute is needed to inhibit the fluid to gel membrane phase transition at low hydration? *Biochim. Biophys. Acta, Biomembr.* **2007**, *1768* (5), 1019−1022.

(11) Gordon-Kamm, W. J.; Steponkus, P. L. Lamellar-to-hexagonal II phase-transitions in the plasma-membrane of isolated protoplasts after freeze-induced dehydration. *Proc. Natl. Acad. Sci. U. S. A.* **1984**, *81* (20), 6373−6377.

(12) Steponkus, P. L. Role of the Plasma Membrane in Freezing Injury and Cold Acclimation. *Annu. Rev. Plant Physiol.* **1984**, *35* (1), 543−584.

(13) Crowe, L. M.; Crowe, J. H. Hydration-dependent hexagonal phase lipid in a biological membrane. *Arch. Biochem. Biophys.* **1982**, *217* (2), 582−587.

(14) Crowe, J. H.; Crowe, L. M.; Oliver, A. E.; Tsvetkova, N.; Wolkers, W.; Tablin, F. The trehalose myth revisited: Introduction to a symposium on stabilization of cells in the dry state. *Cryobiology* **2001**, *43* (2), 89−105.

(15) Sun, W. Q.; Leopold, A. C.; Crowe, L. M.; Crowe, J. H. Stability of dry liposomes in sugar glasses. *Biophys. J.* **1996**, *70* (4), 1769−1776.

(16) Crowe, J. H.; Hoekstra, F. A.; Crowe, L. M. Anhydrobiosis. *Annu. Rev. Physiol.* **1992**, *54*, 579−599.

(17) Lambruschini, C.; Relini, A.; Ridi, A.; Cordone, L.; Gliozzi, A. Trehalose interacts with phospholipid polar heads in Langmuir monolayers. *Langmuir* **2000**, *16* (12), 5467−5470.

(18) Konov, K. B.; Isaev, N. P.; Dzuba, S. A. Low-Temperature Molecular Motions in Lipid Bilayers in the Presence of Sugars: Insights into Cryoprotective Mechanisms. *J. Phys. Chem. B* **2014**, *118* (43), 12478−12485.

(19) Pereira, C. S.; Hunenberger, P. H. Interaction of the sugars trehalose, maltose and glucose with a phospholipid bilayer: A comparative molecular dynamics study. *J. Phys. Chem. B* **2006**, *110* (31), 15572−15581.

(20) Bryant, G.; Wolfe, J. Interfacial forces in cryobiology and anhydrobiology. *CryoLetters* **1992**, *13* (1), 23−36.

(21) Wolfe, J.; Bryant, G. Freezing, Drying, and/or Vitrification of Membrane-Solute-Water Systems. *Cryobiology* **1999**, *39*, 103−129.

(22) Lenné, T.; Garvey, C. J.; Koster, K. L.; Bryant, G. Effects of Sugars on Lipid Bilayers during Dehydration: SAXS/WAXS Measurements and Quantitative Model. *J. Phys. Chem. B* **2009**, *113* (8), 2486−2491.

(23) Demé, B.; Zemb, T. Measurement of sugar depletion from uncharged lamellar phases by SANS contrast variation. *J. Appl. Crystallogr.* **2000**, *33* (3−1), 569−573.

(24) Lenné, T.; Bryant, G.; Garvey, C. J.; Keiderling, U.; Koster, K. L. Location of sugars in multilamellar membranes at low hydration. *Phys. B* **2006**, *385*−*386*, 862−864.

(25) Pincet, F.; Perez, E.; Wolfe, J. Do Trehalose and Dimethyl Sulfoxide Affect Intermembrane Forces? *Cryobiology* **1994**, *31* (6), 531−539.

(26) Yoon, Y. H.; Pope, J. M.; Wolfe, J. The effects of solutes on the freezing properties of and hydration forces in lipid lamellar phases. *Biophys. J.* **1998**, *74* (4), 1949−1965.

(27) Andersen, H. D.; Wang, C.; Arleth, L.; Peters, G. H.; Westh, P. Reconciliation of opposing views on membrane - sugar interactions. *Proc. Natl. Acad. Sci. U. S. A.* **2011**, *108* (5), 1874−1878.

(28) Green, J. L.; Angell, C. A. Phase-Relations and Vitrification in Saccharide-Water Solutions and the Trehalose Anomaly. *J. Phys. Chem.* **1989**, *93* (8), 2880−2882.

(29) Lerbret, A.; Affouard, F.; Hédoux, A.; Krenzlin, S.; Siepmann, J.; Bellissent-Funel, M.-C.; Descamps, M. How Strongly Does Trehalose Interact with Lysozyme in the Solid State? Insights from Molecular Dynamics Simulation and Inelastic Neutron Scattering. *J. Phys. Chem. B* **2012**, *116* (36), 11103−11116.

(30) Lerbret, A.; Bordat, P.; Affouard, F.; Descamps, M.; Migliardo, F. How Homogeneous Are the Trehalose, Maltose, and Sucrose Water Solutions? An Insight from Molecular Dynamics Simulations. *J. Phys. Chem. B* **2005**, *109* (21), 11046−11057.

(31) Magazù, S.; Migliardo, F.; Mondelli, C.; Vadalà, M. Correlation between bioprotective effectiveness and dynamic properties of trehalose−water, maltose−water and sucrose−water mixtures. *Carbohydr. Res.* **2005**, *340* (18), 2796−2801.

(32) Magazu, S.; Migliardo, F.; Ramirez-Cuesta, A. J. Inelastic neutron scattering study on bioprotectant systems. *J. R. Soc., Interface* **2005**, *2* (5), 527−532.

(33) Magazù, S.; Migliardo, F.; Telling, M. T. F. α,α-Trehalose−Water Solutions. VIII. Study of the Diffusive Dynamics of Water by High-Resolution Quasi Elastic Neutron Scattering. *J. Phys. Chem. B* **2006**, *110* (2), 1020−1025.

DOI: 10.1021/acs.langmuir.5b02127
Langmuir 2015, 31, 9134−9141

(34) Bryant, G.; Koster, K. L.; Wolfe, J. Membrane behaviour in seeds and other systems at low water content: the various effects of solutes. *Seed Sci. Res.* **2001**, *11*, 17−25.
(35) Koster, K. L.; Lei, Y. P.; Anderson, M.; Martin, S.; Bryant, G. Effects of vitrified and nonvitrified sugars on phosphatidylcholine fluid-to-gel phase transitions. *Biophys. J.* **2000**, *78* (4), 1932.
(36) Koster, K. L.; Webb, M. S.; Bryant, G.; Lynch, D. V. Interactions between soluble sugars and POPC (1-palmitoyl-2-oleoylphosphatidylcholine) during dehydration: vitrification of sugars alters the phase behavior of the phospholipid. *Biochim. Biophys. Acta, Biomembr.* **1994**, *1193* (1), 143−150.
(37) Kent, B.; Hunt, T.; Darwish, T. A.; Hauss, T.; Garvey, C. J.; Bryant, G. Localization of trehalose in partially hydrated DOPC bilayers: insights into cryoprotective mechanisms. *J. R. Soc., Interface* **2014**, *11* (95), 6.
(38) Al Kayal, T.; Russo, E.; Pieri, L.; Caminati, G.; Berti, D.; Bucciantini, M.; Stefani, M.; Baglioni, P. Interactions of lysozyme with phospholipid vesicles: effects of vesicle biophysical features on protein misfolding and aggregation. *Soft Matter* **2012**, *8* (35), 9115−9126.
(39) Hristova, K.; White, S. H. Determination of the Hydrocarbon Core Structure of Fluid Dioleoylphosphocholine (DOPC) Bilayers by X-Ray Diffraction Using Specific Bromination of the Double-Bonds: Effect of Hydration. *Biophys. J.* **1998**, *74* (5), 2419−2433.
(40) Wiener, M. C.; White, S. H. Fluid Bilayer Structure Determination by the Combined Use of X-Ray and Neutron-Diffraction 0.1. Fluid Bilayer Models and the Limits of Resolution. *Biophys. J.* **1991**, *59* (1), 162−173.
(41) Wiener, M. C.; White, S. H. Fluid Bilayer Structure Determination by the Combined Use of X-Ray and Neutron-Diffraction 0.2. Composition-Space Refinement Method. *Biophys. J.* **1991**, *59* (1), 174−185.
(42) Wiener, M. C.; White, S. H. Structure of a Fluid Dioleoylphosphatidylcholine Bilayer Determined by Joint Refinement of X-Ray and Neutron-Diffraction Data 0.3. Complete Structure. *Biophys. J.* **1992**, *61* (2), 434−447.
(43) Greenspan, L. Humidity Fixed Points of Binary Saturated Aqueous Solutions. *J. Res. Natl. Bur. Stand., Sect. A* **1977**, *81A* (1), 89−95.
(44) Koch, H. J.; Stuart, R. S. The catalytic C-deuteration of some carbohydrate derivatives. *Carbohydr. Res.* **1978**, *67* (2), 341−348.
(45) Koch, H. J.; Stuart, R. S. A novel method for specific labelling of carbohydrates with deuterium by catalytic exchange. *Carbohydr. Res.* **1977**, *59* (1), C1−C6.
(46) Worcester, D. L. Neutron diffraction studies of biological membranes and membrane components. *Brookhaven Symp. Biol.* **1976**, *27*, III37−III57.
(47) Franks, N. P.; Lieb, W. R. The structure of lipid bilayers and the effects of general anaesthetics: An X-ray and neutron diffraction study. *J. Mol. Biol.* **1979**, *133* (4), 469−500.
(48) Schneck, E.; Rehfeldt, F.; Oliveira, R. G.; Gege, C.; Deme, B.; Tanaka, M. Modulation of intermembrane interaction and bending rigidity of biomembrane models via carbohydrates investigated by specular and off-specular neutron scattering. *Phys. Rev. E* **2008**, *78* (6), 061924.
(49) Bracewell, R. N. *The Fourier transform and its applications*; McGraw Hill: New York, 2000.
(50) Caracciolo, G.; Pozzi, D.; Caminiti, R. Hydration effect on the structure of dioleoylphosphatidylcholine bilayers. *Appl. Phys. Lett.* **2007**, *90* (18), 3.
(51) Bryant, G.; Koster, K. L. Dehydration of solute-lipid systems: hydration forces analysis. *Colloids Surf., B* **2004**, *35*, 73−79.
(52) Sum, A. K.; Faller, R.; de Pablo, J. J. Molecular simulation study of phospholipid bilayers and insights of the interactions with disaccharides. *Biophys. J.* **2003**, *85* (5), 2830−2844.
(53) Westh, P. Glucose, sucrose and trehalose are partially excluded from the interface of hydrated DMPC bilayers. *Phys. Chem. Chem. Phys.* **2008**, *10* (28), 4110−4112.
(54) Tian, J.; Sethi, A.; Swanson; Basil, I.; Goldstein, B.; Gnanakaran, S. Taste of Sugar at the Membrane: Thermodynamics and Kinetics of the Interaction of a Disaccharide with Lipid Bilayers. *Biophys. J.* **2013**, *104* (3), 622−632.
(55) Yang, L.; Huang, H. W. A Rhombohedral Phase of Lipid Containing a Membrane Fusion Intermediate Structure. *Biophys. J.* **2003**, *84* (3), 1808−1817.
(56) Koster, K. L.; Lei, Y. P.; Anderson, M.; Martin, S.; Bryant, G. Effects of vitrified and nonvitrified sugars on phosphatidylcholine fluid-to-gel phase transitions. *Biophys. J.* **2000**, *78* (4), 1932−1946.
(57) Crowe, J. H.; Crowe, L. M.; Mouradian, R. Stabilization of Biological-Membranes at Low Water Activities. *Cryobiology* **1983**, *20* (3), 346−356.

DOI: 10.1021/acs.langmuir.5b02127
Langmuir 2015, 31, 9134−9141